P2.52

THE BEHAVIOR OF NUMBER CONCENTRATION TENDENCIES FOR THE CONTINUOUS COLLECTION GROWTH EQUATION USING ONE- AND TWO-MOMENT BULK PARAMETERIZATION SCHEMES

Jerry M. Straka[1], Katharine M. Kanak[2], and Matthew S. Gilmore[3]
[1]School of Meteorology, University of Oklahoma, Norman, Oklahoma
[2]Cooperative Institute for Mesoscale Meteorological Studies (CIMMS), University of Oklahoma, Norman, Oklahoma
[3]Department of Atmospheric Sciences, University of Illinois, Urbana Illinois

1. Introduction

This paper presents a mathematical explanation for the non-conservation of total number concentration N_t of hydrometeors for the continuous collection growth process, for which N_t physically should be conserved for selected one- and two-moment bulk parameterization schemes. Where possible, physical explanations are proposed.

Straka et al. (2005; hereafter S05) evaluated four commonly used parameterization schemes to determine if they would conserve the total number concentration N_t of growing particles when N_t physically should be conserved for processes such as continuous collection growth and vapor diffusion growth. The schemes evaluated are:

- **Scheme A**: one-moment scheme: where q is predicted, n_o is specified as a constant, N_t and D_n are diagnosed,
- **Scheme B**: one-moment scheme: where q is predicted, D_n is specified as a constant, N_t and n_o are diagnosed,
- **Scheme E**: two-moment scheme: where q and D_n are predicted, N_t and n_o are diagnosed, and
- **Scheme F**: two-moment scheme: where q and N_t are predicted, D_n and n_o are diagnosed.

In these schemes, q is mixing ratio, n_o is the slope intercept, and D_n is the characteristic diameter (inverse of the slope of the distribution). S05 found that only scheme-F conserved N_t for vapor diffusion and the continuous collection growth processes for which N_t should be conserved. In this paper, only the continuous collection growth process is considered, for which, it is shown mathematically why N_t is conserved for scheme-F and why N_t is not conserved for the other schemes. Vapor diffusion growth is not shown as the results are qualitatively similar.

In section 2, the relevant equations are presented. In section 3, results are presented for the same set of parameters as those used in S05, except that a smaller initial graupel mixing ratio is used herein in order to have physically meaningful results at later times, such as 600 s. In section 4, it is shown mathematically why N_t is conserved for scheme-F and not conserved for the other schemes. Where possible, the physical bases for these results are proposed. A summary is given in section 5.

2. Equations

The following equations presented below can be found in S05 and elsewhere in numerous references. However it is deemed useful to repeat them so the reader can have quick reference to them to complement the often complex explanations in section 3.

The zeroth moment of a distribution is defined by N_t in units of (m^{-3}) as,

$$N_t = \int_0^\infty n(D)dD \ , \qquad (1)$$

where D is diameter with units (m). The number concentration per unit length is n(D), and is given by a form of the gamma distribution function, e.g.,

$$n(D) = \frac{N_t}{\Gamma(\nu)} \frac{1}{D_n} \left(\frac{D}{D_n} \right)^{\nu-1} \exp\left(-\frac{D}{D_n} \right) \qquad (2)$$

where D_n is the characteristic diameter of the distribution with units (m), $\Gamma(x)$ is the gamma function, and ν is the shape or breadth parameter of the distribution. For hydrometeors that may approximated by spheres, mass can be

written as $m(D) = \alpha D^{\beta}$, where $\alpha = \rho\pi / 6$, and $\beta = 3$. The particle density is denoted by ρ (kg m^{-3}). The third moment, or mixing ratio q, with units of (kg kg^{-1}) can be defined from (2) and the definition of mass for a sphere, which results in an equation relating q, D_n, and N_t,

$$q = \frac{1}{\rho_o}\int_0^{\infty} m(D)n(D)dD = \frac{\alpha N_t \Gamma(\beta+\nu) D_n^{\beta}}{\rho_o \Gamma(\nu)} \quad (3)$$

Solving for D_n results in,

$$D_n^{\beta} = \frac{\rho_o \Gamma(\nu) q}{\alpha N_t \Gamma(\beta+\nu)}. \quad (4)$$

The slope intercept, n_o (units of $m^{-(\beta+\nu)}$), can be found in terms of N_t and D_n

$$n_o = \frac{N_t}{D_n^{\nu}} \quad (5)$$

The sixth moment, or the reflectivity factor Z (for Rayleigh scatterers), for spheres is,

$$Z = \int_0^{\infty} D^{2\beta} n(D)dD = \frac{N_t \Gamma(2\beta+\nu)}{\Gamma(\nu)} D_n^{2\beta} \quad (6)$$

Relating the time rate of change of the third moment (3) with the rate of change of the sixth moment (6), results in an equation (Srivastava 1971, Passarelli 1978, Mitchell 1994) that can be used to derive a prognostic equation for D_n, which is used in scheme-E:

$$\frac{\partial D_{n,x}}{\partial t} = \frac{D_{n,x}}{\beta q_x}\left[\frac{2\Gamma(\beta+\nu+\delta)\Gamma(\beta+\nu)}{\Gamma(\nu+\delta)\Gamma(2\beta+\nu)} - 1\right]\frac{\partial q_x}{\partial t} \quad (7)$$

Rearranging (3) to solve for N_t results in,

$$N_t = \frac{q\rho_o \Gamma(\nu)}{\alpha\Gamma(\beta+\nu) D_n^{\beta}}, \quad (8)$$

Now if the partial derivative of (8) with respect to time t is taken the following equation is found,

$$\frac{\partial N_t}{\partial t} = \frac{\rho_o \Gamma(\nu)}{\alpha\Gamma(\beta+\nu)} \frac{\partial}{\partial t}\left(\frac{q}{D_n^{\beta}}\right). \quad (9)$$

Expanding the derivative and factoring D_n^{β}/q on the right-hand-side of (9) gives,

$$\frac{\partial N_t}{\partial t} = \frac{\rho_o \Gamma(\nu)}{\alpha\Gamma(\beta+\nu)} \frac{q}{D_n^{\beta}}\left(\frac{1}{q}\frac{\partial q}{\partial t} - \frac{\beta}{D_n}\frac{\partial D_n}{\partial t}\right). \quad (10)$$

Conservation of N_t, thus requires the right-hand-side of (10) to equal zero. Thus, the terms in parentheses in (10) must cancel, since none of the terms in front of the parentheses are zero for continuous collection growth. Assuming finite and non-zero q and D_n, which are consistent with continuous collection growth, a conservation condition for N_t may be written as,

$$\frac{1}{q}\frac{\partial q}{\partial t} = \frac{\beta}{D_n}\frac{\partial D_n}{\partial t}. \quad (11)$$

or

Term I = Term II

An alternative way of stating (11) is that the conservation of N_t requires that the time rates of change of ln(q) and βln(D_n) must be equal. Equations (10) and (11) allow the examination of the factors that control the N_t conservation as in scheme–F, or non-conservation as in schemes-A, -B, and -E.

The equations for $\partial q / \partial t$ and $\partial N_t / \partial t$ for continuous collection growth of a spherical solid ice particle (e.g., graupel) are,

$$\frac{\partial q_x}{\partial t} = \frac{\pi E_{x,y} N_{t,x} q_y D_{n,x}^{2.5} \Gamma(2.5+\nu_x)}{4\Gamma(\nu_x)}\left(\frac{4\rho_x g}{3\rho_o C_{d,x}}\right)^{0.5}, \quad (12)$$

and

$$\frac{\partial N_{t,x}}{\partial t} = 0. \quad (13)$$

For each of the four schemes, the time derivatives are evaluated with forward-in-time

differences with a time step of 1 s to permit accurate solutions. The following initial conditions are used for all the schemes in the integrations of (12) and (13):

- q_x = 1 x 10^{-3} kg kg^{-1} initial value for graupel mixing ratio
- Nt = 1000 m^{-3} initial value of total number concentration for graupel particles

The following set of parameters are specified as constants in time and space for all the schemes

- β = 3 for a sphere
- ν = 3 for the distribution shape parameter
- $E_{x,y}$ = 0.55 is the collection efficiency
- ρ_x= 900 kg m^{-3} is the density of graupel
- Cd = 0.60 is the graupeldrag coefficient (12)
- g = 9.8 m s^{-2} is gravity
- q_y = 1.0x10^{-3} kg kg^{-1} is the constant value of mixing ratio for cloud water
- δ = 2.5 in (12) for continuous collection growth

3. Results

Table 1 shows the variables predicted, diagnosed, and/or specified for each scheme and the corresponding equations numbers in parentheses used to obtain the solutions. In addition, the nature of the changes of these variables over the integration period, 600 s, is denoted by an arrow. The length of the arrow represents the relative magnitude of the change with time. A horizontal arrow means the value is constant in time.

Figure 1 shows time series up to 600 s of integration for each of the four variables, N_t, q, D_n, and n_o for each of the four schemes. The time series of N_t for each of the schemes up to t = 600 s is given in Fig. 1a. From both Table 1 and Fig. 1a, it is clear that scheme-F is the only scheme that conserves N_t. The next best is scheme-E, followed closely by scheme-A, though both are non-conservative for N_t. The results of scheme-B are significantly non-conservative for N_t. Thus schemes-A, -E, and especially -B, artificially introduce hydrometeor particles for a process in which N_t should be conserved.

The time series of q for each scheme are shown in Fig. 1b. In all cases the curves are of similar shape and q increases by five to six times its original value. The similar shape of the curves is consistent with the fact that (12) has been used for all the schemes to obtain q (Table 1). Time series of D_n are shown in Fig.1c, in which the characteristic diameter increases for schemes-A, -E, and -F, but does so most strongly for scheme-F. For scheme-B, D_n is specified as constant, and thus does not increase, despite that the process is one of growth in size of graupel particles. Figure 1c thus, demonstrates a physical inconsistency in the design of scheme-B for continuous collection growth or breakup, as the mean diameter nD_n cannot change in time.

Figure 1d shows the slope intercept n_o versus time. Scheme-A includes the specification of n_o as constant (Fig. 1d), which again is a physical inconsistency, as all particles increase in size during growth, and thus, n_o should decrease with time. For schemes-E and -F, n_o does indeed decrease with time. However, for scheme-B, n_o increases rapidly with time according to (4), because D_n is held constant (Fig. 1c and Table 1) and N_t increases rapidly (Fig. 1a). The greatest decrease of n_o with time occurs for scheme-F (Fig. 1d). As the graupel particles get larger overall, they do so more rapidly than with any of the other schemes (Fig. 1c). Using (4) and (5), this behavior of n_o is consistent mathematically, with constant N_t with time (Fig. 1a), increasing q with time (Fig. 1b), and a value of $\frac{1}{D_n^{\nu}}$ that is decreasing with time, as D_n gets larger with time (Fig. 1c).

In summary, Fig. 1a and Table 1 show that scheme-F is the only one to conserve N_t, whilst scheme-B exhibits significantly unphysical results with regard to the conservation of N_t. The performances of schemes-A and -E with regard to N_t conservation are intermediate to scheme-B and -F, but are closer to -F than to -B.

The departure of N_t from conservation can be quantified for this set of parameters and initial conditions, by calculating the relative differences, RD, from scheme-F of each variable, (N_t, q, D_n, and n_o), denoted by y, at 600 s using,

$$RD = \left(\frac{y_{scheme-X} - y_{scheme-F}}{y_{scheme-F}} \right) \times 100 , \qquad (14)$$

where scheme-X is any of schemes-A, -B, or -E. The relative differences are shown in Table 2 for each of the four variables for each scheme. It is clear that scheme-B has the most significant

differences from scheme-F for all the variables. Schemes-A and -E demonstrate non-conservation of N_t, though also with significant relative differences from scheme-F (Table 2), but perform better than scheme-B.

4. Discussion

The conservation properties of N_t of all of the schemes are evaluated using (10). The value of N_t resulting from the integration of (10) holds, within truncation error, for all the schemes, including scheme-F, where N_t is conserved. This means that for the schemes in which N_t is diagnosed at each timestep, the final N_t will give the same value as integrating (10). As far as the authors can tell (10) can be applied to any one- or two- moment scheme and in that sense seems to be general.

To facilitate the demonstration of why scheme-F conserves N_t and schemes-A, -B and -E do not conserve N_t, the terms of equation (10) are decomposed into term I and term II as noted above for (11), and the conservation of N_t is evaluated using the difference of the terms I - II. If the difference is greater than zero, then the value of N_t will unrealistically increase with time, whereas if the difference is less than zero, then the value of N_t will unrealistically decrease with time. Only when the terms cancel each other, is N_t conserved.

Next the detailed behavior of terms I and II (Figs. 2-5) for scheme-F is examined to demonstrate why N_t is conserved. Then schemes-A, -B and -E, are examined to see why N_t is not conserved (Figs. 2-5). Note that in the discussion below, each of the subparts ($1/q$, $\partial q/\partial t$, β/D_n, and $\partial D_n/\partial t$) of terms in I and II are always positive.

a. Scheme-F

Upon examination of term I and its subparts, it is found that while $\frac{1}{q}$ gets smaller with time (Fig. 2a), $\frac{\partial q}{\partial t}$ increases with time (Fig. 2b). This latter term increase is because of the increase in D_n, as N_t is constant with time in accordance with (12) and (13). The term $\frac{1}{q}$ in scheme-F is the largest of any of the other schemes for all times (Fig. 2a), which implies that q is the smallest for scheme-F at all times and this is consistent with Fig. 1b. This occurs even though D_n is the largest for scheme-F. The reason for this behavior is that as q increases with time, N_t does not change with time, thus by (4), D_n increases the most rapidly with scheme-F (Fig. 2c). The net behavior for term I (Fig 4a) is a decrease with time as the term $\frac{1}{q}$ dominates even though $\frac{\partial q}{\partial t}$ increases with time. In term II for scheme-F, the subpart $\frac{\beta}{D_n}$ (Fig 3a), decreases with time, and $\frac{\partial D_n}{\partial t}$ (Fig. 3b) gets larger with time. The net behavior for term II (Fig 4b) is that it decreases with time as the subpart $\frac{\beta}{D_n}$ dominates again over $\frac{\partial D_n}{\partial t}$. Note that the amplitudes and the rates of decrease with time of terms I and II are approximately equal (Fig. 4a,b). The result is such that terms I-II $\approx$ 0, which approximately satisfies the necessary condition (11) for N_t conservation (Fig. 5). In the actual calculation of (10), the slight departure from conservation is less than 0.2% and owes to calculations using numbers with vast differences in order of magnitude.

b. Scheme-A

Term I for scheme-A behaves similarly to scheme-F (Fig. 4a), though term I in scheme-A decreases more slowly with time and thus, is larger at 600 s. This owes to $\frac{\partial q}{\partial t}$ being larger and increasing more quickly in scheme-A than scheme-F (Fig. 2b), and that $\frac{1}{q}$ decreases at about the same rate and is about the same amplitude with both schemes-A and -F (Fig. 2a). Term II decreases with scheme-A (Fig. 4b), like term II with scheme-F, though it is smaller in magnitude than with scheme-F. The difference in magnitude owes to the larger increases in values of $\frac{\partial D_n}{\partial t}$ with time in scheme-F than in

scheme-A (Fig. 3b). The reason for the decreasing term II in scheme-A is that the amplitude of the increasing term $\frac{\partial D_n}{\partial t}$ is less than the amplitude of the decreasing term $\frac{\beta}{D_n}$ (Fig. 3a), which decreases with time but not as much as for scheme-F. As a result of these calculations it is found that I-II > 0 (Fig. 5), which can also be seen in (Fig. 1a) where N_t nearly doubles its initial value in 600 s. Therefore, except for scheme-B, scheme-A performs most poorly with regard to the conservation of N_t, as compared to scheme-F. The relative difference (14) of scheme-A compared to scheme-F is 137 % (Table 2). The large difference owes to the physically inconsistent specification of a constant n_o for the continuous collection growth process.

c. Scheme-B

Examining scheme-B exposes some interesting differences that make this scheme perform very poorly with regard to the conservation of N_t (Fig. 1a and Table 2). First, $\frac{1}{q}$, in term I for scheme-B is slightly smaller than all the other schemes (Fig. 2a). This owes to q being a bit larger than with any other scheme (Fig. 1b). This does not result from the constant D_n being large in (4), rather that it is too small (Fig. 1c) and that there associated very large values of N_t with scheme-B. The values, of $\frac{\partial q}{\partial t}$ in term I (Fig. 2b), are much larger than any of the other schemes. Again, this is not a direct result of the smaller values of D_n, but rather of much larger values of N_t, which are indirectly forced by the small, specified constant D_n (8). Term II (Fig. 4b) simply is zero as D_n is constant with time, i.e., $\frac{\partial D_n}{\partial t}$ = 0 (Fig. 3b). This is the physical basis for non-conservation with scheme-B. That is, the characteristic diameter is not allowed to increase during a growth process with increasing q, and this results in N_t being forced to be quite large according to (8) and (10), as term II (which is zero) cannot possibly offset term I (Fig. 4). Thus, terms I-II > 0 (Fig. 5). Note, however, that $\frac{\beta}{D_n}$ is larger with scheme-B than with any other scheme (Fig 3a). This owes again to D_n being too small and specified as a constant. Finally, n_o also is increasing (Fig. 1d) rapidly with time with this scheme, when it should decreasing physically like scheme-F. This is a result of rapidly increasing values of N_t and a small, but constant D_n in (5). The result of a diagnosis using (8) and prediction using (10) gives a N_t that has a relative difference of more than 500% from scheme-F by 600 s (Table 2). Therefore, this scheme has the largest relative differences compared to scheme-F or any of the schemes (Table 2), and is the most unphysical, as it forces unrealistic production of particles for a process in which there should not be any production of new particles, as well an unphysical behavior for D_n and n_o for this growth process.

d. Scheme-E

Finally, scheme-E is the second best performing scheme with regard to N_t conservation. Term I is larger than in scheme-F at 600 s (Fig. 4a), while at 600 s, term II is smaller as compared to scheme-F (Fig. 4b). In term I, $\frac{1}{q}$ decreases slightly more with scheme-E than with scheme-F (Fig. 2a). This means that $\frac{\partial q}{\partial t}$ must increase more than with scheme-F (Fig. 2b), which is indeed the case. With scheme-E, D_n has the second largest value of all the schemes (Fig. 1c), so $\frac{\beta}{D_n}$ is closer to scheme-F than any other scheme (Fig. 3a). With scheme-E, term II decreases with time owing to $\frac{\beta}{D_n}$ decreasing more rapidly (Fig. 3a) than $\frac{\partial D_n}{\partial t}$ is increasing (Fig. 3b). The end result is then is that terms I-II > 0 (Fig. 5), which makes the prediction of N_t with (11) non-conservative and the relative difference using (14) is > 100 % (Table 2).

In general, term II changes more with

time than term I for all the schemes, except for scheme-B where terms I and II are approximately constant (Fig. 4). The time series of term I - term II (Fig. 5), as calculated from (11) for each scheme, are consistent with the results in Table 2 and Fig. 1, with regard to the conservation of N_t. Scheme-B has the worst performance while schemes-A and -E have intermediate performance. The difference of term I - term II is positive for schemes -A, -B, and -E, which indicates that particles are artificially added during this continuous collection growth process in which N_t should physically be conserved.

5. Summary

By dissecting the terms in (10), or equivalently (11), which is a conservation condition for N_t based on the partial time derivative of the definition of the third-moment, it is possible to explain why only scheme-F, the two-moment scheme which predicts q and N_t, is conservative for N_t when it should be for certain microphysical processes like continuous collection growth (and vapor diffusion growth. [not shown – see S05]). These equations (10) and (11) also explain why the other schemes are non-conservative.

The assumption of a constant n_o in scheme-A is physically inconsistent with the continuous collection growth process, as is the assumption of a constant D_n for scheme-B. In order to compensate for these inappropriate assumptions, the other variables obtained with these schemes are also often inaccurate in order to compensate. Scheme-E is also non-conservative but it seems this result is not owing to a physically inconsistent specification, but rather the solutions scheme's equations simply do not satisfy N_t conservation.

It is crucial that numerical model users be aware of the physical behavior of these schemes in order that they may properly interpret their model output when simulating these and other similar microphysical processes using bulk parameterizations. The recommendation is consistent with that in S05, that scheme-F, should be used instead of the other schemes in order to preserve physical realism to the greatest extent possible by conservation of N_t.

Acknowledgements: This work was supported by the National Science Foundation (NSF) grants, ATM-0340639, and ATM-0339519. K. Kanak is supported by the Cooperative Institute for Mesoscale Meteorological Studies (CIMMS) under award NA17RJ1227 from the NOAA, U.S. Department of Commerce, and NSF ATM-0135510.

REFERENCES

Mitchell, D. L., 1994: A model predicting the evolution of ice particle size spectra and radiative properties of cirrus clouds. Part I: Microphysics. *J. Atmos Sci*., **51**, 797-816.

Passarelli, R. E., 1978: An approximate analytical model of the vapor deposition and aggregation growth of snowflakes. *J. Atmos Sci*., **35**, 118–124.

Srivastava, R. C., 1971: Size distributions of raindrops generated by breakup and coalescence. *J. Atmos. Sci*., **28**, 410-415.

Straka, J. M., M. S. Gilmore, K. M. Kanak, and E. N. Rasmussen, 2005: A comparison of the conservation of number concentration for the continuous collection and vapor diffusion growth equations using one- and two-moment schemes. *J. Appl. Meteor*., **44**, 1844-1849.

Scheme	q	N_t	D_n	n_o
A	P (12)	D (8) E (10)	D (4) E (FD)	S
B	P (12)	D (8) E (10)	S	D (5)
E	P (12)	D (8) E(10)	P (7)	D (5)
F	P (12)	P (13) E (10)	D (4) E (FD)	D (5)

Table 1. Variables used in each of the four schemes A-F with the associated equation in parentheses by which they are computed, where **P = Predicted, D=Diagnosed, and S=Specified as constant**. The qualitative change in these terms with time is indicated by an arrow. The length of the arrow corresponds roughly to the relative amount of change in 600 s of integration. In some cases there are horizontal arrow-heads that indicate the values are constant in time. In addition to the equations in parentheses that are used to solve for the variables, in some cases these values are compared to the values obtained using either a simple finite difference **FD** between t = 0 and t = 600 s or through the use of equation (10) and these are labeled **E = examined**. The finite difference is calculated using $\partial(D_n)/\partial t \approx (D_n^{n+1} - D_n^n)/\Delta t$.

Scheme	q	N_t	D_n	n_o
A	11.40	136.53	22.20	402.28
B	26.76	536.70	41.61	3097.97
E	8.98	99.07	18.20	263.62
F	0.00	0.00	0.00	0.0

Table 2. Relative differences, RD, (in percent) of the solutions for q, N_t, D_n, and n_o for each scheme relative to scheme-F as calculated using (14) at t = 600 s.

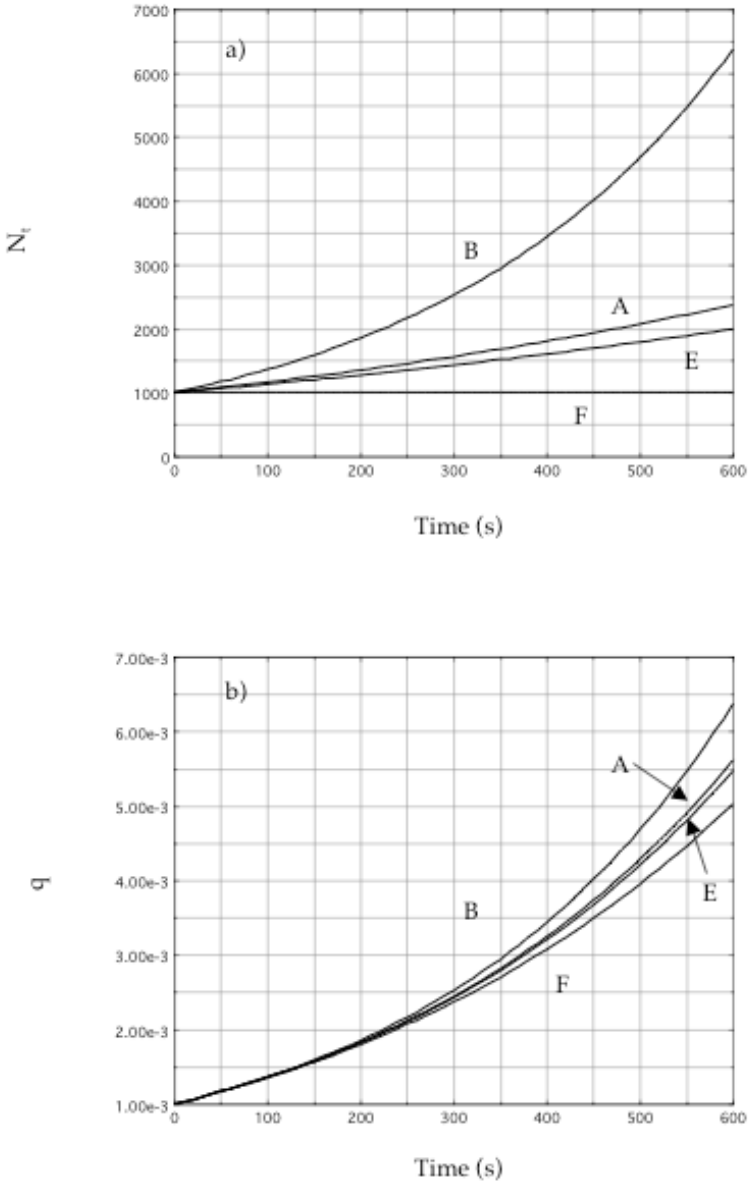

Fig. 1. Time series up to 600 s. a) N_t in units of (m^{-3}) vs. time (s). b) q in units of (kg kg^{-1}) vs. time (s).

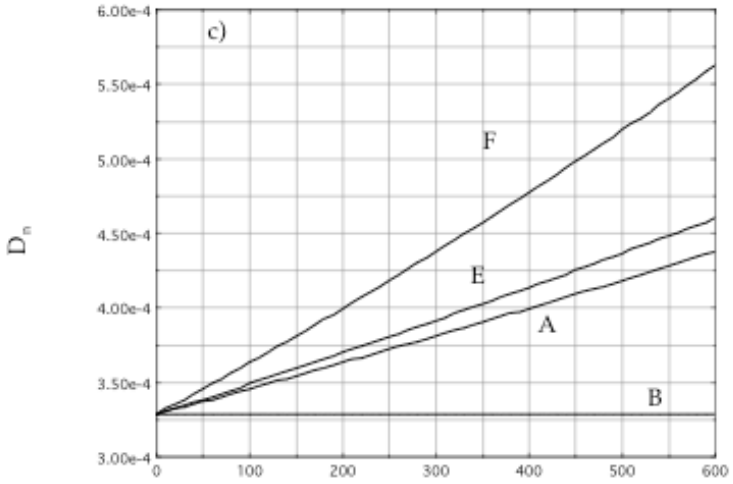

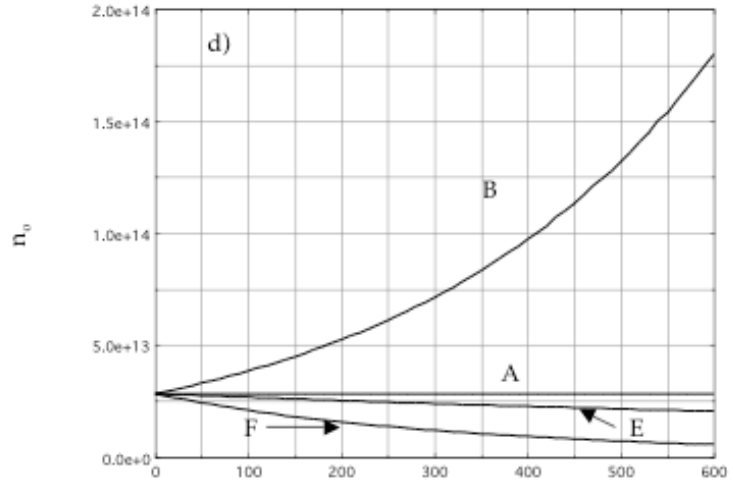

Fig. 1 continued. Time series up to 600 s. c) D_n in units of (m) vs. time (s). d) n_o in units of ($m^{-(\beta+\nu)}$) vs. time (s).

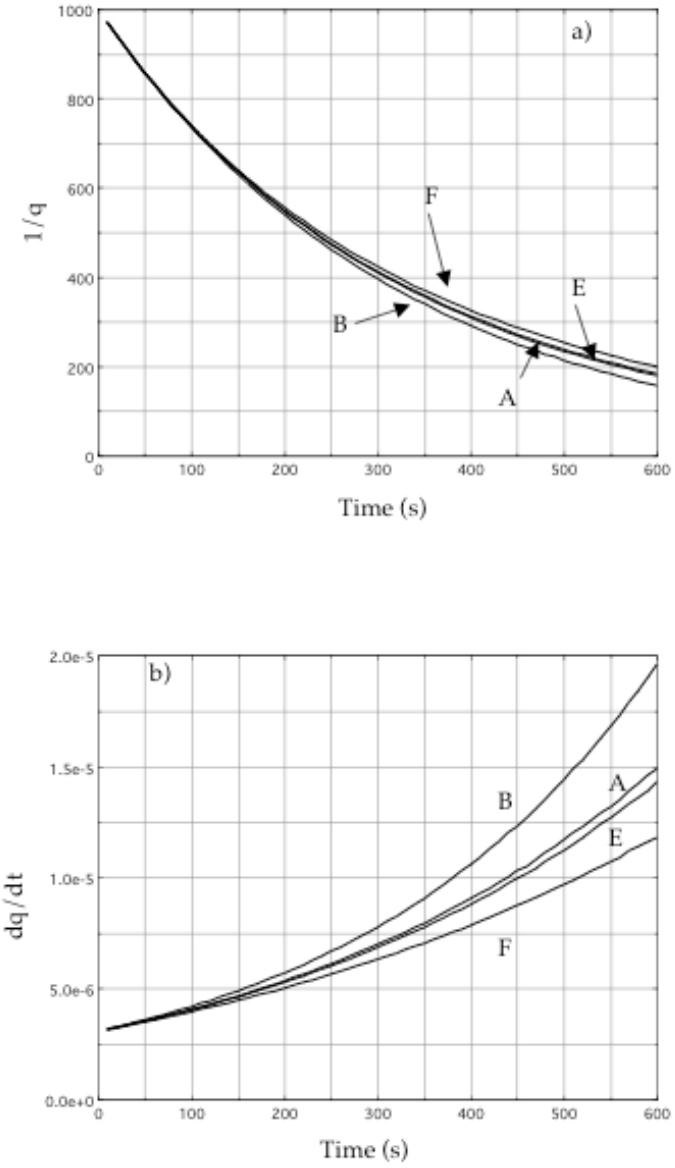

Fig. 2. Time series up to 600 s of subparts of the term I from (11). a) $1/q$ in units of (kg kg^{-1}) vs. time (s). b) $\partial q/\partial t$ in units of (kg kg^{-1} s^{-1}) vs. time (s).

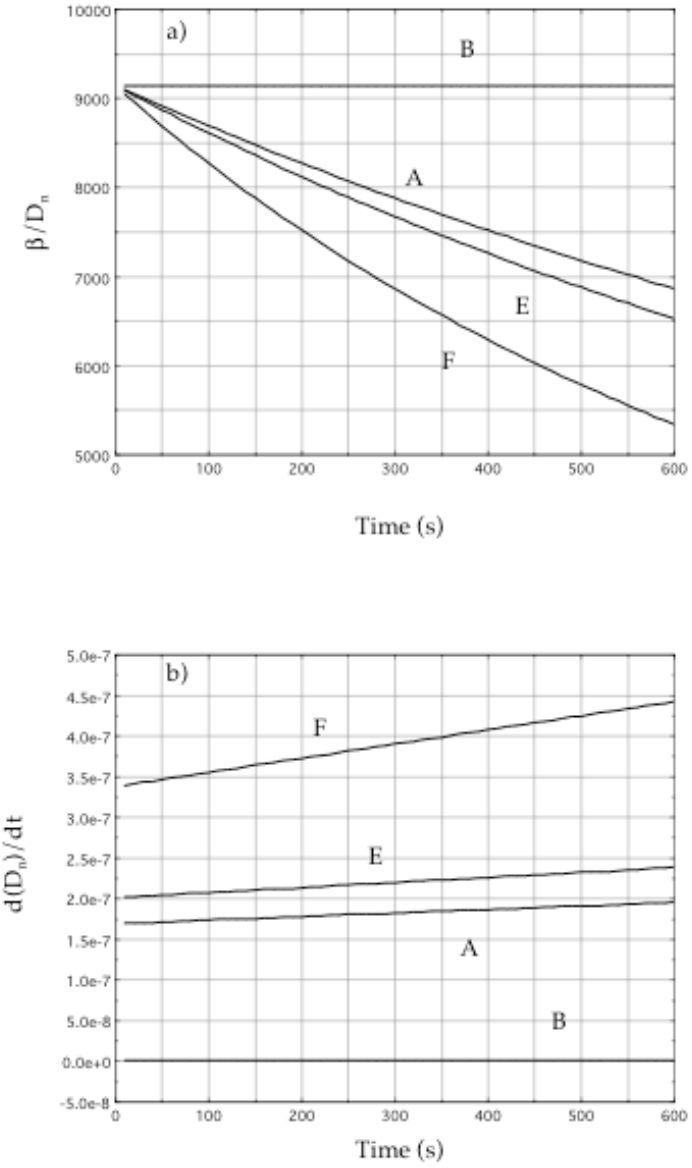

Fig. 3. Time series up to 600 s of subparts of the term II from (11). a) β/D_n in units of (m^{-1}) vs. time (s). b) $\partial(D_a)/\partial t$ in units of ($m\ s^{-1}$) vs. time (s).

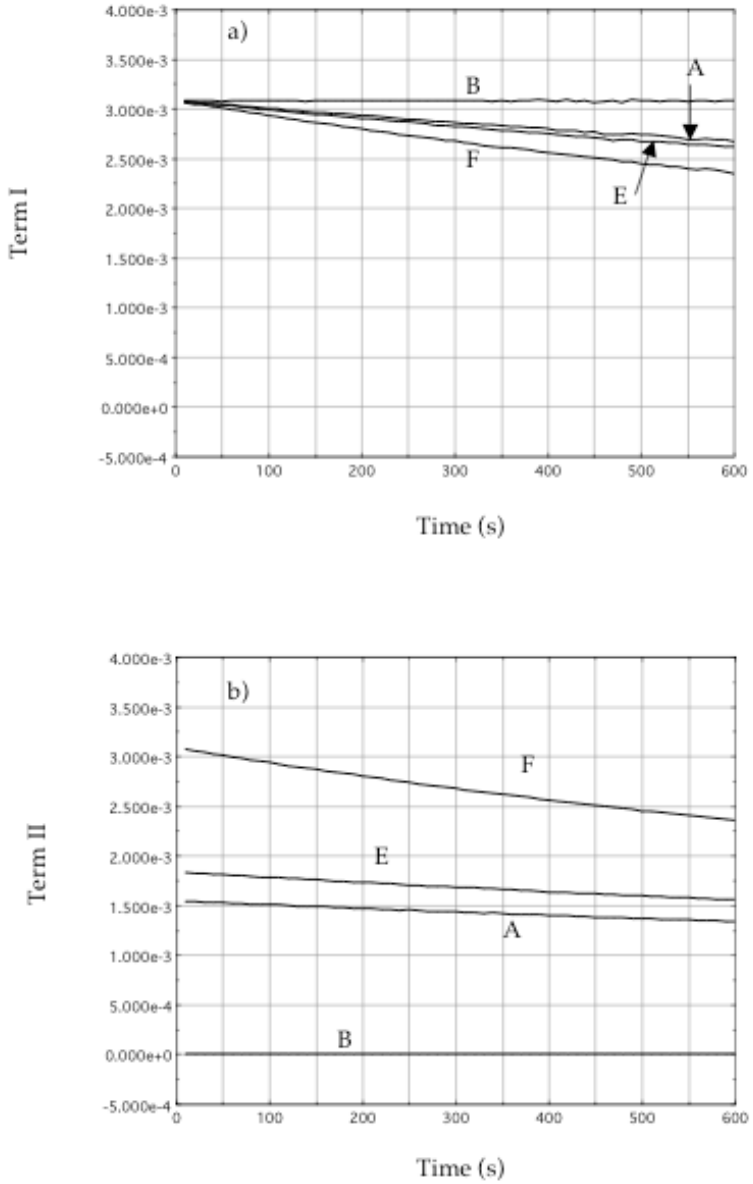

Fig. 4. Time series up to 600 s of the terms from (11). a) Term I = $(1/q)(\partial q/\partial t)$ in units of (s^{-1}) vs. time (s). b) Term II = $(\beta/D_n)(\partial(D_n)/\partial t)$ in units of (s^{-1}) vs. time (s).

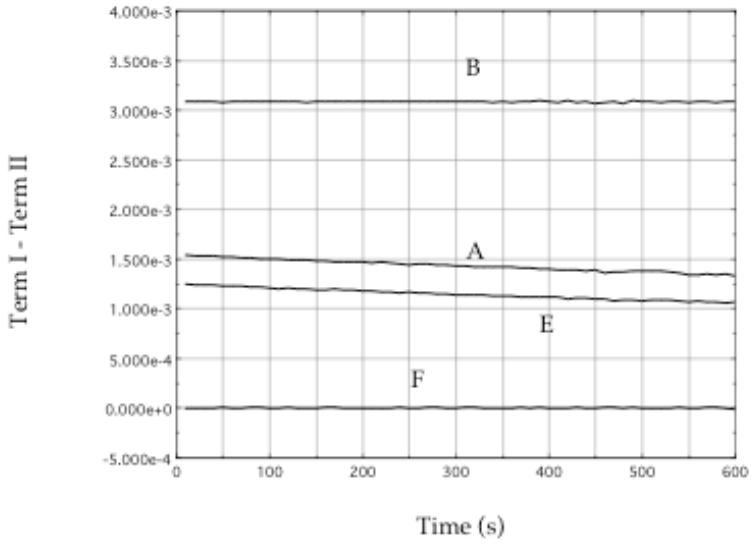

Fig. 5. Time series up to 600 s of the difference of the terms (I - II) from (11). Term I -Term II = $[(1/q)(\partial q/\partial t) - (\beta/D_n)\partial(D_n)/\partial t)]$ in units of (s^{-1}) vs. time (s).